Spring 2022

Development and Kinetic Survey of a G148T Mutant Human Cytosolic Malate Dehydrogenase Isoform 3 Enzyme with Oxaloacetate and A-ketoglutarate

Ethan N. Dionne

Development and kinetic survey of a G148T mutant human cytosolic malate dehydrogenase isoform 3 enzyme with oxaloacetate and α-ketoglutarate

Initially Submitted May 18, 2021; Revised January 2022 for Publication

Ethan N. Dionne, Lorenzo Battistoni, Tyler Stack, and Kathleen Cornely

From the Providence College Department of Chemistry and Biochemistry, Providence, RI, USA

Cancer cells often use an altered metabolic pathway in which glycolysis, uncoupled from the citric acid cycle, serves as the primary source of ATP. To support cancer cell proliferation and growth, the glycolytic enzyme glyceraldehyde-3-phosphate dehydrogenase (GAPDH) must have a constant source of NAD. While lactate dehydrogenase (LDH) in its conversion of pyruvate to lactate is a well-known source of cytosolic NAD for GAPDH activity, cytosolic malate dehydrogenase (MDH1) also plays a role in cell proliferation through its generation of cytosolic NAD by the conversion of OAA to malate. This development has implicated MDH1 in cancer cell metabolism and characterizing the interactions of its different isoforms with alternate substrates serves as a potential route to cancer treatments. In this study, we created a G148T mutant of human cytosolic malate dehydrogenase isoform 3 (hMDH1) using site-directed mutagenesis to survey potentially altered substrate specificity with oxaloacetate (OAA) and α-ketoglutarate (αKG). We produced a sample of both the mutant enzyme and the wild type enzyme (WT hMDH1) by overexpression in *Escherichia coli* and purification by Ni-NTA affinity chromatography. We assessed the purity of the enzyme samples using SDS-PAGE and determined the protein concentration of each sample using a bicinchoninic acid (BCA) assay. We performed kinetics assays of the G148T hMDH1 mutant with OAA αKG to determine enzyme activity relative to the wild type using a modified Michaelis Menten model. This study demonstrates that the G148T hMDH1 mutant enzyme has decreased turnover rate and proficiency with OAA compared to the wild type enzyme and that αKG is likely not a viable substrate for hMDH1 isoform 3.

The enzyme malate dehydrogenase (MDH) reversibly catalyzes the redox conversion of malate and oxaloacetate (OAA) with the co-substrate NAD/NADH. At least two forms of MDH exist in most eukaryotes: a mitochondrial form (MDH2) which functions as the last step of the citric acid cycle, and a cytosolic form (MDH1) which is involved primarily with the malate/aspartate shuttle, which exchanges reducing equivalents in the form of malate and aspartate across the mitochondrial membrane (1,2). The two forms have a relatively low extent of primary structure similarity, with only 19.6% identity between mitochondrial and cytosolic porcine MDH, and the enzyme systems can function independently from one another (1,3,4). Both forms of MDH generally exist as dimers, and each subunit contains two domains: an NAD-binding domain and a substrate binding domain (1). In addition to malate and OAA, citrate is also known to bind to the substate binding domain as an inhibitor of the enzyme (1). Different isoforms of each type of MDH exist, and characterizations of these different isoforms are currently underway through an MDH course-based undergraduate research experience (CURE) program of which this research is associated (5).

Cytosolic MDH has recently been implicated in the proliferation of cancer cells, which typically have altered metabolism, relying heavily on glycolysis uncoupled from the citric acid cycle to sustain cell growth and division (4). To sustain glycolysis, a steady supply of cytosolic NAD is necessary, which acts as an electron acceptor and cofactor in the reaction catalyzed by glyceraldehyde-3-phosphate dehydrogenase (GAPDH). Generation of NAD for this reaction has been known to come from lactate dehydrogenase (LDH), which converts pyruvate to lactate, however, an alternative source of cytosolic NAD has been shown to also come from MDH1 (4). Deuterium labeling studies conducted by Hanse *et al.* revealed that malate is a significant hydrogen bond acceptor during cell proliferation, and that MDH1 knockout cells proliferated more slowly and consume less glucose than cells with functional MDH1. In addition, studies indicate that MDH1 is amplified in solid tumor cancer cells (4).

Malate dehydrogenase enzymes are known to be highly selective for OAA and malate as substrates, and rational,

single amino acid mutations have been applied as a strategy to manipulate MDH substrate specificity (3). These studies have demonstrated the importance of residue composition and structural conformation of the active site, including a flexible loop region covering the active site, for selection of alternative substrates such as α-ketoglutarate (αKG) (3). In this study, one such rational, single amino acid mutation is made to human cytosolic malate dehydrogenase isoform 3 (hMDH1) with the site-directed mutagenesis of glycine at position 148 in the wild-type hMDH1 isoform 3 enzyme (EC: 1.1.1.37; Uniprot: P40925-3) to a threonine. This mutation yielded a viable, soluble enzyme, and enzyme kinetics relative to the wild type hMDH1 (WT hMDH1) indicated that the G148T mutant hMDH1 showed decreased activity with the OAA substrate compared to the WT hMDH1 while both the wild type and the mutant showed little to no activity with αKG as an alternative substrate.

Results

Visualization of hMDH1

Potential targets for site-directed mutagenesis were identified using a multiple sequence alignment. The sequence alignment included 29 different MDH protein sequences spanning a diverse selection of organisms. Conserved residues across all MDH proteins from the alignment were not considered for mutation. In the interest of influencing hMDH1 substrate specificity, potential mutations were considered around a flexible loop region near the active site on which, many charged, hydrophilic residues extend outward. The residues located on the loop (Figure 1, yellow) are highly conserved across MDH enzymes and are thought to have an effect on the enzyme's likelihood of binding substrate from the cytosol (3). The conformation of the loop also directly influences the size of the active site (3). The residue glycine 148 (Figure 1*A*,*B*, magenta) was hypothesized to be a promising location for mutation due to its location immediately adjacent to the active site loop (Figure 1*B*). Changing a glycine for a larger residue was hypothesized to shift the loop region and potentially increase the size of the active site. With this logic, a threonine at the 148 position (Figure 1*C*, magenta) was introduced in PyMol to visualize what might happen to the loop region (6). While there is not currently a structure for cytosolic human MDH (hMDH1), the conformational changes that might be induced by a G148T mutant are depicted in porcine MDH (Figure 1, PDB code 5MDH), which has 95.5% identity (Uniprot) to human MDH.

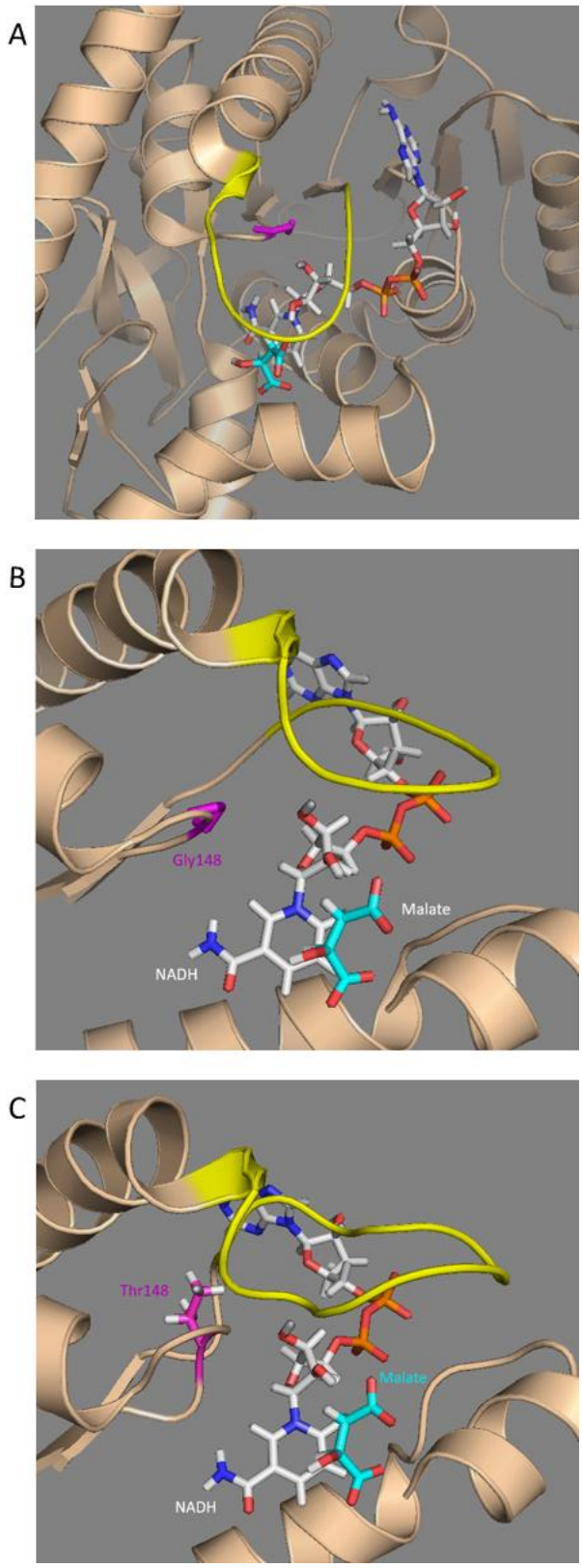

Figure 1. Proposed mutation at residue 148. *A*, A view of the alpha subunit of hMDH1 isoform 3, providing a macroscopic view of MDH, the position of the loop (yellow), the binding sites of NADH (white) and malate (cyan) substrates, as well as residue 148 (magenta). *B*, A view of the wild type enzyme with glycine at residue 148. *C,* The proposed G148T mutant. The larger threonine residue at position 148 changes the conformation of the active site loop.

Preparation of pET28a plasmid vector

Before proceeding with site-directed mutagenesis, preparation of an expression vector containing the hMDH1 isoform 3 gene was necessary. This process was expedited with the generous gift of a pET28a plasmid containing the hMDH1 isoform 3 gene from Dr. Jessica Bell and colleagues at the University of San Diego. The plasmid was isolated from *E. coli* BL21(DE3) cells with a yield of 125 ng/µL and a 260/280 ratio of 1.96 (Figure 2), which falls within the typical range of 1.8-2.0 for pure DNA (7). The 260/230 ratio was slightly high for DNA at 2.45 from an expected range between 2.0-2.2, potentially indicating inconsistencies between the pH or ionic strength of the blanking solution compared to the sample solution (8). The isolated pET28a vector containing hMDH1 was used as a template in site-directed mutagenesis PCR.

Site-directed mutagenesis

The nucleotides that corresponded to glycine 148 were located and primers were designed to introduce the mutation to threonine with the altered codon ACT from the wild type glycine codon GGT through PCR. The PCR product was visualized using agarose gel electrophoresis to confirm the presence of an intact plasmid containing the hMDH1 gene (Figure 3). The expected amplicon for the pET28a plasmid is present at 6292 bp, suggesting that the site-directed mutagenesis primers successfully annealed to the substrate and likely introduced the desired point mutation. The PCR product was then circularized by kinase, ligase, DpnI (KLD) treatment. The kinase in the treatment first phosphorylates the 5' ends of the plasmid, then ligase seals gaps in the plasmid's DNA phosphodiester backbone for circularization. Finally, the endonuclease DpnI degrades any remaining non-mutated template DNA in the mixture (9). The circularized, KLD treated plasmid was successfully transformed into NEB 5-alpha *E. coli* cells (Figure 4). Many colonies are visible against the Luria Bertani (LB) and kanamycin solid culture medium, indicating that the pET28a plasmid vector containing a kanamycin resistance gene was successfully transformed into the cells. The pET28a plasmid containing the putative G148T hMDH1 mutant gene was then isolated with a yield of 40 ng/µL (Figure 5). The 260/280 ratio of this plasmid sample is slightly greater than desired at 2.15 (optimal between 1.8-2.0), however, this does not indicate any issues with sample quality. The 260/230 ratio is very high, although still acceptable as this does not usually indicate the presence of contaminants (7). The identity of the plasmid sample was determined using Sanger sequencing (Genewiz), which indicated successful introduction of the G148T mutation.

Overexpression and purification of hMDH1

Purified protein samples of both the wild type hMDH1 and the G148T mutant hMDH1 enzymes were prepared for downstream kinetics assays. The isolated pET28a expression vectors for the wild type and G148T mutant hMDH1 isoform 3 protein were each transformed into Zymo Research *E. coli* Xjb (DE3) cells for overexpression.

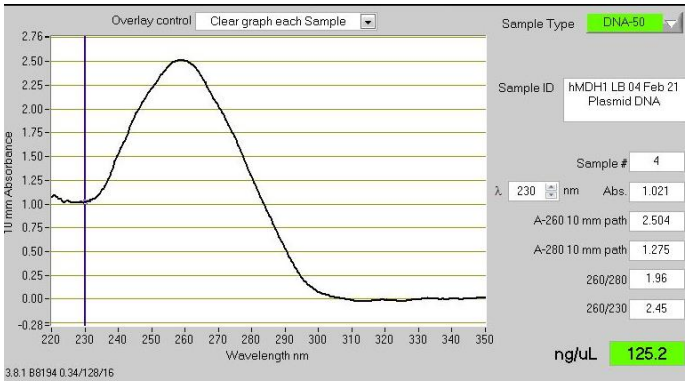

Figure 2. Absorbance spectrum of isolated pET28a vector containing wild type hMDH1. A distinct peak is visible at 260 nm, indicating a pET28a DNA sample of good quality. The sample is relatively concentrated at 125 ng/µL.

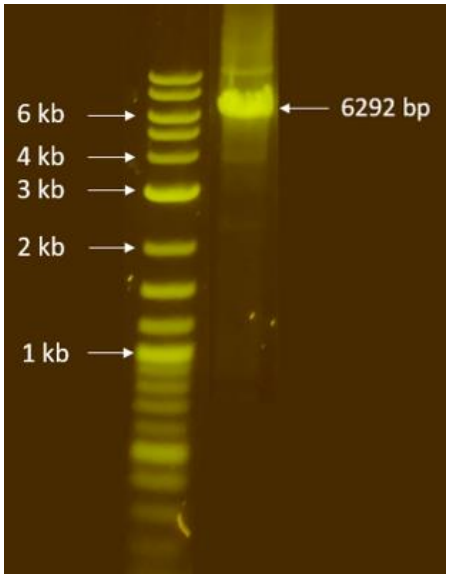

Figure 3. Gel electrophoresis of site-directed mutagenesis PCR product. This gel indicates the presence of the pET28a expression vector containing the hMDH1 gene. While this gel does not indicate successful introduction of the G148T mutation, the intensity of the band at 6292 bp suggests that the site-directed mutagenesis primers successfully annealed to the substrate and likely introduced the desired G148T mutation. The gel also demonstrates that the PCR mixture does not contain significant quantities of smaller molecular weight DNA fragments.

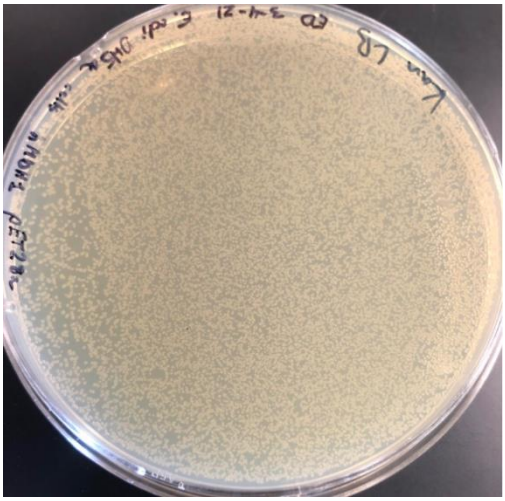

Figure 4. Transformation into NEB *E. coli* 5-alpha cells. Many colonies are present on the LB + kanamycin plate. This indicates that the cells contain the pET28a plasmid with the kanamycin resistance gene, indicating successful transformation.

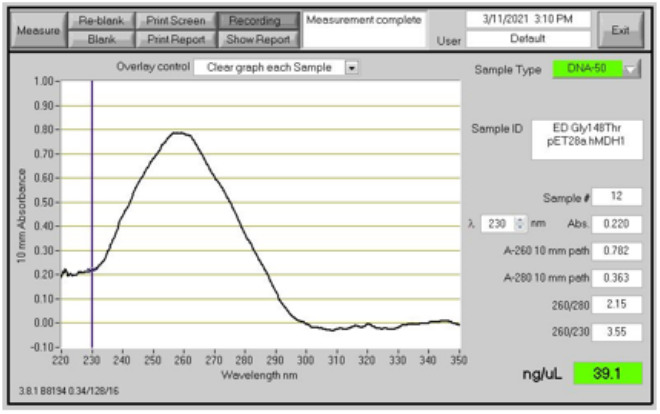

Figure 5. Absorbance spectrum of isolated pET28a vector containing G148T mutant hMDH1. The sample appears free of contaminants with an expected 260/280 ratio for DNA. The sample has an acceptable concentration at 40 ng/µL for downstream applications. This sample was successfully sequenced and its identity as pET28a containing the G148T mutant hMDH1 gene was confirmed.

The transformation efficiency of the cells containing the G148T mutant hMDH1 gene was 62.5 CFU/µg DNA (Figure 6). Single colonies from each transformation were picked and cultured overnight in an LB + kanamycin liquid medium, then expanded. Overexpression of the target enzymes and autolysis of cells was induced, then the wild type and G148T mutant hMDH1 enzymes were each purified from the Xjb cell lysate by Ni-NTA affinity chromatography. The Ni-NTA ligand of the column's solid phase adheres to a histidine tag added to the carboxy terminus of the protein by the pET28a expression vector. Washes with 25 mM imidazole followed by elution with 250 mM imidazole yielded the desired protein. The lysate, flowthrough, washes, and eluent were each assessed for the presence of the target protein by SDS-PAGE (10) (Figure 7*A*). The lysate (Mut Lys) contained a complex mixture of cellular proteins, including the overexpressed target protein. The flowthrough (Mut FT, WT FT) contained most of the cellular proteins with no significant indication of target protein. The wash (Mut Wash) contained a small amount of protein that had weak or partial affinity to the column, while the eluent (Mut Elu, WT Elu) contained a concentrated amount of the purified protein with minimal contaminants (Figure 7*A*). The Benchmark ™ prestained protein ladder was also used to determine the molecular weight of the overexpressed WT hMDH1 protein and the G148T hMDH1 mutant protein. To do this, the square root of the molecular weight of the ladder was plotted as a function of the log of the distance migrated down the gel (Figure 7*B*). This generated a standard curve from the protein ladder that could be used to determine the molecular weight of the overexpressed hMDH1 proteins by measuring the distance traveled in the gel. Using this method, the molecular weight of the WT hMDH1 was determined to be 32.1 kDa and the molecular weight of the G148T hMDH1 mutant was determined to be 31.6 kDa. This differed from molecular weights determined in silico (Benchling), which calculated a theoretical molecular weight of 39.7 kDa for both enzymes.

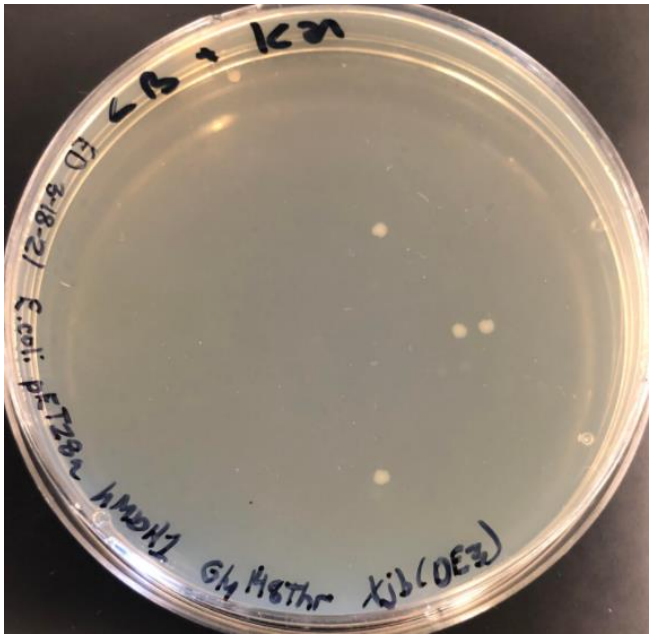

Figure 6. Transformation of pET28a containing the G148T mutant hMDH1 enzyme into Zyme *E. coli* Xjb (DE3) cells. Five colonies are present on the LB + kanamycin plate. Although the transformation was successful, this indicates low transformation efficiency.

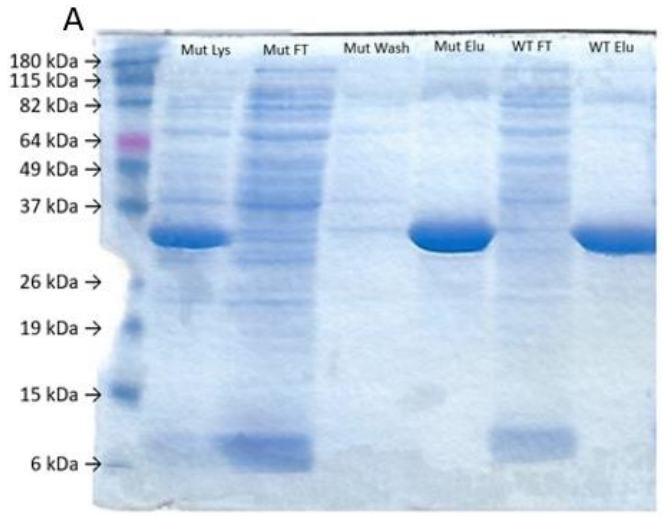

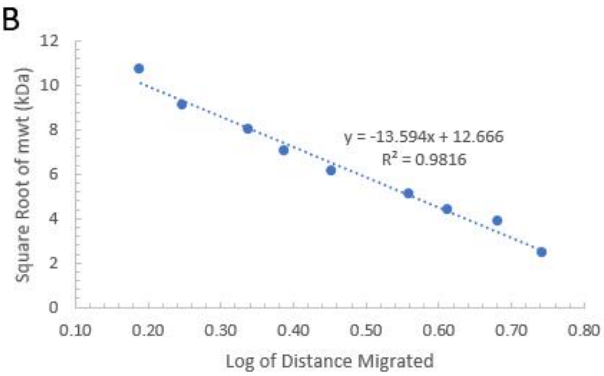

Figure 7. SDS-PAGE. *A,* The protein composition of different phases of the protein purification process by Ni-NTA affinity chromatography. *B,* The standard curve generated by the protein ladder to determine molecular weight of WT hMDH1 and the G148T hMDH1 mutant.

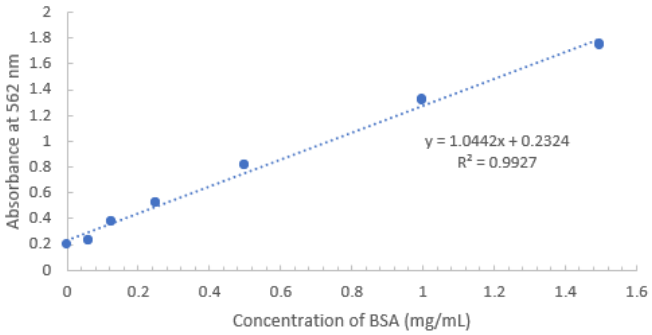

Figure 8. BCA assay standard curve. The standard curve was constructed from BSA standards with known concentrations.

BCA assay

The protein concentration of WT hMDH1 and G148T mutant hMDH1 eluent samples were each determined by a bicinchoninic acid (BCA) assay (11). A set of standards was prepared from bovine serum albumin (BSA) and the absorbance was measured at 562 nm. The protein concentration of the hMDH1 eluent samples were determined using the BSA standard curve (Figure 8). The concentration of the wild type hMDH1 eluent sample was determined from an average of 6 assays done in triplicate for an average of 0.61 mg/mL. The concentration of the G148T mutant hMDH1 eluent, determined from a single set of triplicate samples was 0.75 ± 0.01 mg/mL.

Enzyme Kinetics

The kinetic constants k_{sp}, k_{cat}, and K_M for the WT hMDH1 and G148T mutant hMDH1 were each determined (Table 1) from the observed rate of conversion from OAA to malate with the consumption of NADH (k_{obs}). The consumption of NADH was monitored spectrophotometrically by absorbance at 340 nm. The observed rate as a function of OAA substrate concentration was then plotted and fit using a modified Michaelis Menten equation (12) (Figure 9*A,B*). The alternative substrate α-ketoglutarate (αKG) was also surveyed for activity with both the WT hMDH1 and the G148T hMDH1 mutant, and the kinetic constants are reported (Table 1). The observed rate as a function of αKG substrate concentration was also determined from the change in absorbance at 340 nm (Figure 9*C,D*).

Table 1

Kinetic constants for WT hMDH1 and the G148T mutant hMDH1 with native substrate OAA and alternate substrate αKG

	k_{cat} (s^{-1})	k_{sp} ($\mu M^{-1} s^{-1}$)	K_M (μM)
WT OAA	**320 ± 10**	**18 ± 2**	**18 ± 2**
G148T OAA	**2.3 ± 0.1**	**0.038 ± 0.002**	**60 ± 4**
WT αKG	**0.4 ± 0.2**	**{70 ± 900,000}**	**{0.005 ± 70}**
G148T αKG	**0.2 ± 0.1**	**{80 ± 2.0 × 10^7}**	**{0.003 ± 500}**

Discussion

This study has successfully generated a single amino acid mutation in hMDH1 isoform 3 (G148T) and surveyed its activity with the substrates OAA and αKG relative to the WT hMDH1. The goal of site-directed mutagenesis with hMDH1 was to make a targeted, rational amino acid mutation and assess consequent substrate activity and specificity. The replacement of glycine at position 148 with a bulkier threonine residue was designed to change the conformation of the active site and flexible loop region which closes over the active site (Figure 1). This loop region is highly conserved across MDH enzymes and is thought to significantly affect substrate binding in solution (3).

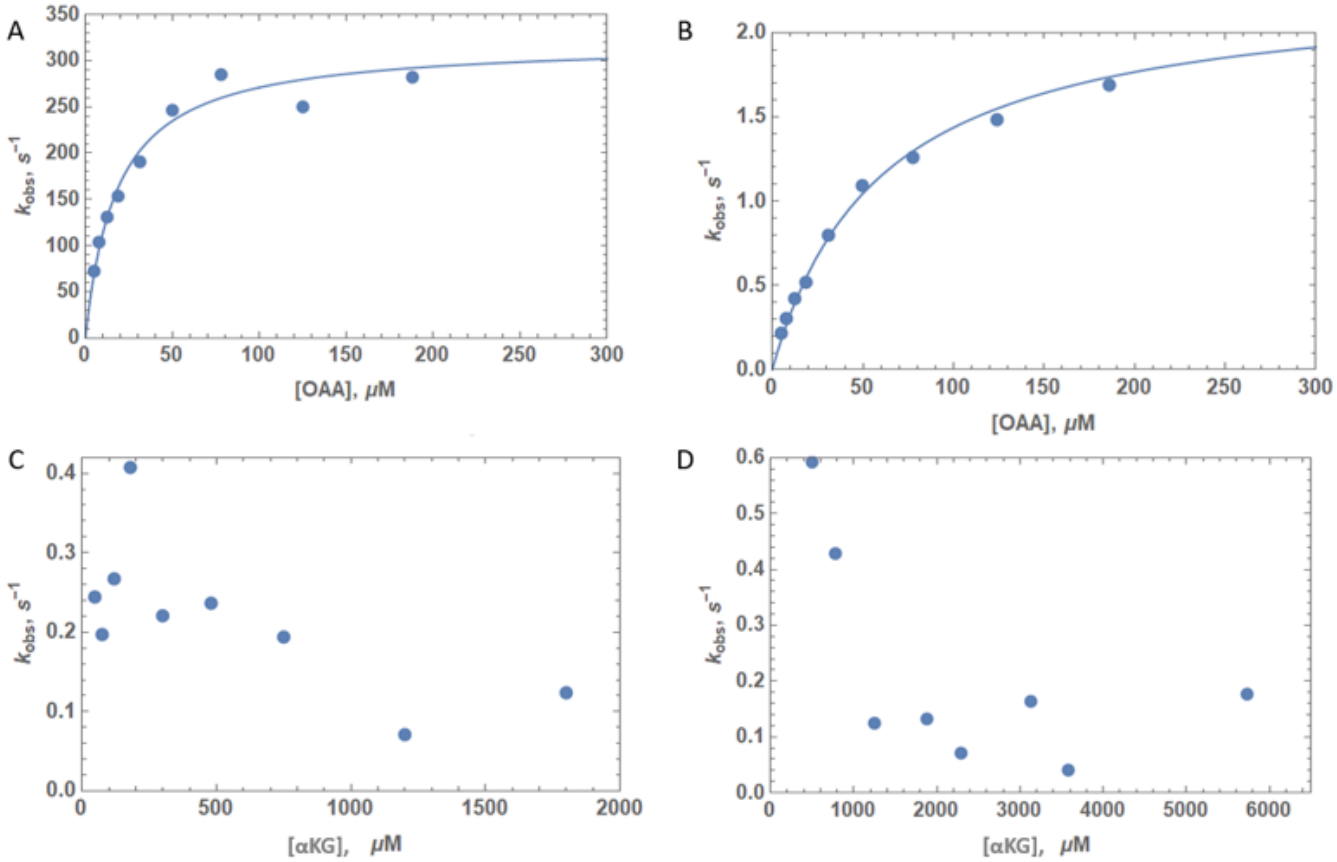

Figure 9. Kinetics traces. *A,* The observed reaction rate for WT hMDH1 as a function of OAA concentration. *B*, The observed reaction rate for the G148T hMDH1 mutant as a function of OAA concentration. *C*, The observed reaction rate for the WT hMDH1 as a function of αKG concentration. *D,* The observed reaction rate for the G148T hMDH1 mutant as a function of αKG concentration.

All results related to site-directed mutagenesis, subsequent transformations, protein overexpression, and purification indicate the successful creation of the intended G148T hMDH1 mutation. With the 6292 bp amplicon indicating an intact pET28a vector containing the hMDH1 gene, the agarose gel electrophoresis following site-directed mutagenesis PCR indicated successful annealing of the mutagenesis primers to the substrate pET28a vector containing the WT hMDH1 gene (Figure 3). Circularization of the linear PCR product by KLD treatment and transformation into NEB 5-alpha *E. coli* cells also suggested success because the solid media is supplemented with kanamycin and colonies only form with the presence of the pET28a vector which contains a kanamycin resistance gene (Figure 4). The plasmid was isolated from the NEB 5-alpha cells with acceptable purity (a 260/280 ratio of 2.15) and concentration at 40 ng/μL (Figure 5). Sequencing of the plasmid (Genewiz) confirmed the successful codon swap from GGT to ACT, which encode glycine and threonine, respectively. Transformation of the pET28a expression vector containing the desired mutation into *E. coli* Xjb cells was also successful, albeit with low transformation efficiency at 62.5 CFU/μg of DNA (Figure 6). Subsequent overexpression of MDH, cell lysis, and protein purification by affinity chromatography were also successful as indicated by SDS-PAGE with the different eluents from Ni-NTA affinity chromatography (Figure 7*A*). The lanes labeled "Mut Elu" and "WT Elu", each show the purified samples containing the G148T hMDH1 mutant enzyme and WT hMDH1, respectively. These lanes each show an intense band around 32 kDa, which matches the approximate molecular weight of hMDH1, which Benchling analysis predicts at ≈ 40 kDa and Uniprot reports as 38.6 kDa. A more precise determination of the molecular weight of the proteins was an analysis of the gel using the protein ladder as a standard curve (Figure 7*B*). This method was used to determine a molecular weight of 31.6 kDa for the mutant hMDH1, and 32.1 kDa for the WT hMDH1. This apparent 6-8 kDa discrepancy between the

predicted molecular weight might be ameliorated by a smaller amount of protein loaded on the gel, which might produce a less intense band that could be more precisely measured relative to a protein ladder of known molecular weight. With the purified protein present in the sample, a BCA assay was performed to determine its concentration. Using the standard curve of BSA standards, the protein concentration of the G148T hMDH1 mutant sample was determined as 0.75 ± 0.01 mg/mL while an average for the concentration of the WT hMDH1 sample was determined as 0.61 mg/mL from a larger dataset.

The activity of the WT hMDH1 sample and the G148T hMDH1 mutant were assessed using the substrates OAA and αKG, yielding mixed results. For WT hMDH1 with OAA, k_{cat} was determined as 320 ± 10 s^{-1}, k_{sp} was 18 ± 2 μM^{-1} s^{-1}, and K_M was 18 ± 2 μM. These results set a baseline for the activity of the native enzyme but appear much lower than some literature values which report a k_{cat} around 780 s^{-1} (2,13). The G148T hMDH1 mutant had a much lower turnover rate than the WT, with k_{cat} at 2.3 ± 0.1 s^{-1} and a lower specificity with k_{sp} at 0.038 ± 0.002 μM^{-1} s^{-1}. This lower turnover and specificity manifests in the K_M, which was approximately 3 times greater than the K_M of the wild type at 60 ± 4 μM. This result indicates that the G148T mutant was less efficient at converting OAA to malate with the consumption of NADH than the WT enzyme. These results demonstrate agreement with the hypothesis that the threonine mutation at position 148 would change the conformation of the active site and influence enzyme function and substrate specificity.

The alternative substrate αKG produced inconclusive results with the kinetics assays performed on both the WT and mutant hMDH1 enzymes. Malate dehydrogenase has inherently strong specificity for OAA and malate as substrates, and although αKG has previously been described as an alternative substrate for MDH, its observed reaction rate is noted as 10,000-fold less than with OAA (2,3). The kinetics assay conducted in this study was not refined enough to appreciably represent this difference in the activity. The k_{cat} values for both the WT hMDH1 and the G148T hMDH1 mutant were close to zero, at 0.4 ± 0.2 s^{-1} and 0.2 ± 0.1 s^{-1}, respectively, each with 50% error. The remaining kinetic values were associated with tremendous amounts of error and were inconclusive (Table 1). To detect MDH activity with the αKG alternative substrate, the assay conditions will need to be refined to obtain optimal precision for detection of activity 10,000-fold less than with OAA. This would include further manipulation of substrate and enzyme concentrations in the assay to obtain the best possible absorbance changes over time. However, in only considering the data presented here, it appears that αKG is not a viable substrate for hMDH1 isoform 3.

A potential source of error with the αKG kinetics assay was the presence of a contaminant species which also absorbed at 340 nm. Upon addition of the αKG substrate to the assay mixture, absorbance increased sharply from 0.8 to 1.2, and an absorbance spectrum of the αKG stock solution indicated a weakly absorbing species with a peak at 320 nm (data not shown). Further investigation of this phenomenon might be necessary to obtain precise kinetic data for αKG, as other chemical species in the assay mixture might interfere with the absorbance signal.

Relative to the broad goals of this research, further work must be done to conclusively determine the effect of the G148T hMDH1 mutation. It is evident that this mutation changed the active site conformation of the enzyme, decreasing the enzyme's proficiency to convert OAA to malate, but the mutation's effect on substrate specificity is still unknown with the inconclusive result of kinetic assays with αKG. Future studies might define the optimal conditions for kinetics using αKG or investigate additional alternative substrates or inhibitors of the enzyme. Inhibition of mutated MDH enzymes might be particularly relevant in relation to cancer, as specificity for an inhibitive alternative substrate might provide valuable data to develop cancer treatments by stunting cancer cell glucose metabolism with decreased availability of cytosolic NAD for the glycolytic enzyme GAPDH (4).

Experimental Procedures

Preparing liquid cultures

Liquid cultures were inoculated from *E. coli* BL21(DE3) cells containing hMDH1 isoform 3 streaked on a plate generously provided by Dr. Jessica Bell at the University of California San Diego. Cells were grown up in Luria-Bertani (LB) medium pH 7.5 (1% tryptone, 0.5% yeast extract, 1% NaCl) with 50 μg/mL kanamycin using a baffled flask. Cultures were grown for 14-22 hours at 28°C shaking 250 rpm.

Plasmid isolation from E. coli

Cultures of *E. coli* BL21(DE3) with a pET28a plasmid containing the hMDH1 isoform 3 gene were grown to an OD_{600} between 4-6. A 3 mL volume of *E. coli* cells were pelleted and resuspended in water before processing. The Zymo Research Zyppy Plasmid Miniprep kit was used for

the remaining plasmid isolation and instructions were followed as provided by Zymo. An additional centrifugation of 16,000 × g for 4 minutes was done after adding neutralization buffer to account for puffy protein precipitate. Another additional centrifugation of 13,000 × g was done to remove any residual Zyppy Wash buffer before elution. Elution was done with 10 mM Tris pH 7.5 prewarmed to 50°C and allowed to incubate on the Zymo spin column for 20 minutes before centrifugation to elute. The concentration of plasmid DNA was measured using the Thermo Scientific Nanodrop™ 1000 Spectrophotometer.

Site-directed mutagenesis

To introduce the G148T mutation, site-directed mutagenesis of hMDH1 isoform 3 on the pET28a expression vector was done using the Q5® Site-Directed Mutagenesis Kit (New England BioLabs). Amino acid mutations were codon optimized for *E. coli* and introduced by PCR with complementary primers designed using NEBaseChanger (New England BioLabs). In the PCR mixture, 25 ng of pET28a DNA was used as the template with the forward primer `TATTGTTGTGactAATCCAGCCAATACC` and the reverse primer `ACCTTAACTGACTTCTTG`, where lowercase nucleotides in the forward primer represent alterations for the desired codon change from glycine to threonine. The following PCR protocol was used: 98°C initial denaturation for 30 seconds, 30 cycles of 98°C denaturation (10 seconds), 56°C annealing (30 seconds), and 72°C extension (2 minutes 30 seconds), followed by a final extension of 72°C for 2 minutes. The result of the reaction was visualized on a 1% agarose gel in TBE (89 mM Tris, 89 mM boric acid, 2 mM EDTA) precast with SYBRsafe (Invitrogen). Quick Load® Purple 1kb Plus DNA Ladder (New England BioLabs) was used as a reference to identify amplicons. The hMDH1 DNA sequence containing the G148T mutation introduced by PCR was then treated with KLD reaction buffer and KLD enzyme mix provided with the Q5® Site-Directed Mutagenesis Kit (New England BioLabs). The KLD treatment was done to circularize the linear PCR product containing the G148T mutation. The KLD treated, circularized plasmid was then transformed into chemically competent NEB® High Efficiency DH5α *E. coli* cells (New England BioLabs) for replication of pET28a containing the hMDH1 G148T mutation. The KLD mixture was added to the cells and placed on ice for 30 minutes. The cells were then heat shocked at 42°C for 30 seconds. Following heat shock, the cells were placed on ice for 5 minutes, then combined with room temperature SOC media (2% vegetable peptone, 0.5% yeast extract, 10 mM NaCl, 2.5 mM KCl, 10 mM $MgCl_2$, 10 mM $MgSO_4$, 20 mM glucose) and incubated at 37°C for 1 hour shaking 250 rpm. Cells were pelleted by centrifugation at 3,000 × g for 3 minutes and resuspended in 100 µL of water. The resuspension was then cultured on solid LB medium (3% agar) containing 50 µg/mL kanamycin. The plate was incubated at 37°C overnight. A resulting colony was then picked and expanded in a liquid culture with LB and 50 µg/mL kanamycin. The plasmid was then isolated and sequenced (Genewiz) to confirm the plasmid's sequence identity with the intended G148T mutant sequence prior to protein overexpression.

Protein overexpression

For both the wild type hMHD1 isoform 3 plasmid and the G148T hMDH1 isoform 3 mutant, the pET28a expression vectors were transformed into *E. coli* Xjb (DE3) cells (Zymo Research, product # T3051). Cells were thawed on ice, 40 ng of DNA was added, and cells were incubated on ice for 10 minutes. Following incubation on ice, 4 volumes of SOC medium were added and the cells were incubated for 1 hour shaking at 150 rpm. Cells were pelleted by centrifugation at 3,000 × g for 3 minutes, supernatant was discarded, and the pellet was resuspended in 100 µL of medium. The resuspension was plated on LB supplemented with 50 µg/mL kanamycin and incubated at 37°C overnight. A resulting colony was propagated in liquid LB medium with 50 µg/mL kanamycin at 37°C shaking 250 rpm overnight, then expanded to an OD_{600} of 0.5-0.6. Protein expression and autolysis were induced by addition of IPTG to a concentration of 0.5 mM and arabinose to a concentration of 3 mM, respectively. Cells were grown overnight at 20°C shaking 250 rpm and harvested the next day by centrifugation at 3,000 × g and 4°C for 10 minutes. The resulting pellet was frozen at -20°C.

Cell lysis and affinity chromatography

After overexpression, frozen *E. coli* Xjb (DE3) cells were thawed on ice, then refrozen with liquid nitrogen and rethawed on ice. This introduced an additional freeze-thaw cycle. The cells were then resuspended in a volume of lysis buffer (20 mM Tris, 100 mM NaCl, pH 8.0) based on cell weight (3 mL/g). The lysis buffer was supplemented with a Pierce™ Protease Inhibitor tablet (Thermofisher, A3255), 1 mg of lysozyme, and 30 units of DNAse I (VWR, 0649-50KU). The mixture was incubated at 37°C shaking 200 rpm for 30 minutes to facilitate resuspension

and cell lysis. The cell lysate was then pelleted by two rounds of centrifugation at 21,130 × g and 4°C for 5 minutes. The pellet was discarded, and supernatant lysate was mixed with an equal volume of equilibration buffer (PBS, 20 mM sodium phosphate, 300 mM sodium chloride, pH 7.4) and a 2 mL bed of Ni-NTA resin by end-over-end rotation for 30 minutes at 4°C. The resulting slurry was added to a glass column and the flow through was collected. Following the initial flow through, washes consisting of PBS (phosphate-buffered saline: 20 mM sodium phosphate, 300 mM sodium chloride, pH 8) with 25 mM imidazole were done until the absorbance at 280 nm was less than 0.100, at which point hMDH1 was eluted from the column using 3 resin bed volumes of PBS containing 250 mM imidazole. The hMDH1 eluent was then dialyzed using dialysis membrane tubing (Spectra/Por, 12,000-14,000 molecular weight cutoff) in dialysis buffer (10 mM potassium phosphate, 0.1 mM EDTA, pH 8.0) stirring at 4°C. Fresh dialysis buffer was applied twice, once after 20 hours, and the second time after 70 hours.

BCA Assay

To determine the concentration of hMDH1 protein samples, a bicinchoninic acid (BCA) assay for the colorimetric detection and quantification of protein was performed (11). This was done using the Pierce™ BCA Protein Assay Kit (Product #23209) using the test-tube protocol at room temperature as described in the product user guide. All volumes listed in the test-tube protocol were reduced by half.

SDS-PAGE

The purity of the WT hMDH1 and G148T mutant hMDH1 eluent samples were assessed by SDS-PAGE as described previously (10) with minimal changes. A 4% acrylamide stacking gel and a 12% acrylamide separating gel were made. The sample buffer was prepared using 0.03125 M Tris, 1% SDS, 12.5% glycerol, and 0.005% bromophenol blue. Samples were added to sample buffer and boiled for 5 minutes to dissociate proteins. A volume of sample was loaded on the gel to deliver between 5-100 ng of protein, and wells were topped off with Tris/glycine reservoir buffer (0.025 M Tris, 0.192 M glycine and 0.1% SDS, pH 8.3) (10). The samples were loaded on the gel and the gel was run at a constant 200 volts for 45 minutes. The gel was then stained in Coomassie Blue staining solution (0.025% Coomassie Blue R-250, 40% methanol, 7% acetic acid) overnight. The gel was destained by repeated washing with water and heating in a microwave, then by repeated washing in destaining solution (40% methanol, 7% acetic acid, 3% glycerol) while shaking. The destained gel was then dried using a vacuum gel dryer.

Enzyme Kinetics Assay

The kinetics of both the WT hMDH1 and the G148T mutant hMDH1 sample were assessed spectrophotometrically by tracking the consumption of NADH over 10 seconds at 340 nm. For the WT hMDH1, enzyme to a final concentration of 1 nM, NADH to a final concentration of 0.13 mM, and OAA to varying concentrations between 0.005-0.313 μM were added to a 3000 μL volume of potassium phosphate buffer (100 mM, pH 7.5). The change in absorbance over time was monitored with different concentrations of OAA, and the reaction velocity as a function of OAA substrate concentration was plotted using a modified Michaelis Menten equation (12). The kinetic constants, k_{sp}, k_{cat}, and K_M were then determined from the equation below.

$$v = \frac{k_{SP}[S]}{1 + k_{SP}[S]/k_{cat}}$$

Where

$$K_M = \frac{k_{cat}}{k_{sp}}$$

In the equation above, v is the reaction velocity, [S] is the concentration of substrate, k_{cat} is the maximum turnover (k_{cat}) and proficiency of the enzyme (k_{cat}/k_{uncat}), and k_{sp} is the specificity and efficiency of the enzyme (k_{cat}/K_M).

A kinetics assay of an alternative substrate α-ketoglutarate (αKG) was also performed. The concentration of NADH was spectrophotometrically monitored at 340 nm over a period 20 seconds. For the WT hMDH1, enzyme to a final concentration of 204 nM, NADH to a final concentration of 0.14 mM, and αKG to varying concentrations between 48-3000 μM were added to a 3000 μL volume of potassium phosphate buffer. The change in absorbance over time was monitored with different concentrations of αKG, and the reaction velocity as a function of αKG substrate concentration was plotted using the modified Michaelis Menten equation above. The kinetic constants, k_{sp}, k_{cat}, and K_M were also determined for the WT hMDH1 and the G148T hMDH1 mutant enzymes. The data was processed and plotted using Mathematica.

Acknowledgements – We graciously thank the Department of Chemistry and Biochemistry at Providence College and Department Chair, Dr. Kenneth Overly, for support and

budget allowances for this project. We also thank the Providence College Department of Biology, especially Dr. Brett Pellock, for supporting this project and sharing laboratory equipment essential for completion of these experiments. We thank Dr. Jessica Bell at the University of California San Diego for the generous gift of the pET28a plasmid containing the hMDH1 isoform 3 sequence. For data contributions to WT hMDH1 sample and enzyme concentration, as well as WT hMDH1 with αKG kinetic data, we thank Colby Agostino, Erica Cates, Katelyn Hino, Leah McCarthy, Lily Lockhart, Sophia Moniodes, Sophia Pantazelos, and Francis Radics. We thank the MDH CURE Community (MCC) for inviting Providence College to participate in this research project. Finally, we thank Dr. Joeseph Provost for developing MDH models.

References

1. Minárik, P., Tomásková, N., Kollárová, M., and Antalík, M. (2002) Malate dehydrogenases--structure and function. *Gen. Physiol. Biophys.* **21,** 257-265
2. Wright, S. K., and Viola, R. E. (2001) Alteration of the Specificity of Malate Dehydrogenase by Chemical Modulation of an Active Site Arginine. *J. Biol. Chem.* **276,** 31151-31155
3. Goward, C. R., and Nicholls, D. J. (1994) Malate dehydrogenase: A model for structure, evolution, and catalysis. *Protein. Sci.* **3,** 1883-1888
4. Hanse, E. A., Ruan, C., Kachman, M., Wang, D., Lowman, X. H., and Kelekar, A. (2017) Cytosolic malate dehydrogenase activity helps support glycolysis in actively proliferating cells and cancer. *Oncogene.* **36,** 3915-3924
5. Bell, J., Provost, J., and Bell, E. (2020) The Evolution of the Malate Dehydrogenase CUREs Community. *FASEB. J.* **34,** 1
6. The PyMOL Molecular Graphics System, Version 1.7.4.5 Schrödinger, LLC.
7. Matlock, B. (2015) Assessment of Nucleic Acid Purity (**2021)** *Thermo Fisher Scientific Inc.*
8. Wilfinger, W. W., Mackey, K., and Chomczynski, P. (1997) Effect of pH and Ionic Strength on the Spectrophotometric Assessment of Nucleic Acid Purity. *BioTechniques.* **22,** 474-481
9. Siwek, W., Czapinska, H., Bochtler, M., Bujnicki, J. M., and Skowronek, K. (2012) Crystal structure and mechanism of action of the N6-methyladenine-dependent type IIM restriction endonuclease R.DpnI. *Nucleic acids research.* **40,** 7563-7572
10. Laemmli, U. K. (1970) Cleavage of Structural Proteins during the Assembly of the Head of Bacteriophage T4. *Nature.* **227,** 680-685
11. Smith, P. K., Krohn, R. I., Hermanson, G. T., Mallia, A. K., Gartner, F. H., Provenzano, M. D., Fujimoto, E. K., Goeke, N. M., Olson, B. J., and Klenk, D. C. (1985) Measurement of protein using bicinchoninic acid. *Anal. Biochem.* **150,** 76-85
12. Johnson, K. A. (2019) New standards for collecting and fitting steady state kinetic data. *Beilstein. J. Org. Chem.* **15,** 16-29
13. Talaiezadeh, A., Shahriari, A., Tabandeh, M. R., Fathizadeh, P., and Mansouri, S. (2015) Kinetic characterization of lactate dehydrogenase in normal and malignant human breast tissues. *Cancer. Cell. Int.* **15,** 19